A novel axial passive magnetic bearing design for a self-bearing motor

Cao Hung Ta[1], Dac Anh Ngo[1], Trong Tuan Vu[1], Anh Quan Pham Doan[1], Trung Tuyen Bui[1,2,*],
Van Nam Giap[1], Quang Dich Nguyen[1]

[1]Hanoi University of Science and Technology
[2]Vinh University of Technology Education
*Corresponding author E-mail: Tuyen.BT230003D@sis.hust.edu.vn
DOI: https://doi.org/10.64032/mca.v30i1.392

Abstract

This paper introduces a novel axial passive magnetic bearing (APMB) design tailored for self-bearing motors. The proposed configuration uniquely enables the generation of both attractive and repulsive magnetic forces within a unified structure, contingent upon the rotor's axial displacement. This dual-force capability contributes to enhanced rotor stability and effectively mitigates torque disturbances arising from non-coaxial axial force couples acting on the motor shaft. A comprehensive parametric analysis is conducted to evaluate the influence of key design variables on the bearing's levitation force and stiffness characteristics. Finite Element Analysis (FEA) simulations substantiate the bearing's ability to produce bidirectional axial forces and reveal the sensitivity of levitation performance to variations in design parameters along both axial and radial directions. Additionally, the paper presents a detailed design methodology to guide the practical implementation of the proposed APMB architecture.

Symbols

Symbols	Units	Description
r_{r1}, r_{r2}	mm	Outer and inner diameters of rotor magnet 1
r_{s1}, r_{s2}	mm	Outer and inner diameters of stator magnet 1
D_1, D_2	mm	Thickness of rotor magnet 1 and stator magnet 3
D_3, D_4	mm	Thickness of rotor magnet pair 2 and 3, stator magnet pair 1 and 2
L_1, L_2	mm	The width magnets rotor 3 and stator 3
G	mm	Air gap between rotor and stator
F_z, F_r	N	Axial and radial lifting forces
k_z, k_r	N/mm	Axial and radial stiffness
z, r	mm	Axial and radial air gap displacement
z_{cb}	mm	Magnetic bearing equilibrium position
$\mathfrak{R}_i$	H^{-1}	Magnetic reluctance of the i-th magnetic circuit
$\mathcal{F}_i$	A	Magnetomotive force of the i-th magnet
W_f	J	Magnetic field energy
W_m	J	Mechanical energy
W_l	J	Loss energy
W_e	J	Electric field energy
Φ	Wb	Magnetic flux in the air gap

1. Introduction

Self bearing motor is an electrical motor with the support of the magnetic to levitate the rotor instead of using the mechanical ball bearing, which can reduce the friction loss and avoid the utilization of the lubricant [1]. To obtain the complete self-levitating bearing motor, the mechanical joints must be completely replaced by the magnetic bearing. However, in recent years, the self-bearing motor has been designed which is functioned in certain degree of freedom. Therefore, the self-bearing motors must be embedded together with the auxiliary magnetic bearing to handle the other degree of freedoms in the motor control system. In [2-3], two positive magnetic bearings for controlling the horizontal position of the motor were introduced. In [4] horizontal self bearing motor was introduced with the positive magnetic bearing for controlling the axial position. In [5-6], the proof of the stability of the rotor under the control of the magnetic forces were given in detail. However, to obtain the goal of levitation, the energy consumption can be increased [7]. Especially, in the vertical magnetic bearing, the energy is strongly consumed due to the gravity force levitating. For improving the efficiency, the hybrid magnetic bearing was introduced. Therein, the passive magnetic bearing was used for the generation of the levitation force while the active magnetic bearing is in charge of stabilizing the position of the motor. Basically, the passive magnetic bearing is obtained by using the permanent magnets. Therefore, the energy consumption is eliminated. In [8], the validation of the energy reduction and the efficiency improvement by using the passive magnetic bearing was given. However, according to the Earnshaw law, the operation of the passive magnetic bearing is limited by the fixed flux. Therefore, as the magnetic force is uncontrollable, a motor with full degree of freedom with embedded passive magnetic bearing is an undoable task [9]. So for that crucial reason, the passive magnetic bearing can be created in some certain degree of freedom which is suitable for the self bearing motor with the aim of reducing the energy consumption and the control system size and also the computation complexity. There are two main kinds of

passive magnetic bearings such as the attractive and repulsive passive magnetic bearings [10-11]. The passive magnetic bearing with attractive function is less commonly use than it is in the repulsive format due to the reason that the stiffness coefficients of these types of bearing are respectively defined to be positive and negative. The positive coefficient denotes the variation in the same direction of the force and the displacement, which causes difficulties in calculating and designing the working position. For which reason, the passive magnetic bearing with repulsive ability is preferred. The conventional method is that the same pole of magnet is used to generate the repulsive force, which can be found in [11-12]. This method offers the benefit of being straightforward to apply. However, the magnets flux cannot completely close, which makes the computation of levitate force and operating point becomes remarkably challenging. The novel conical magnetic bearing for flywheel was introduced in [13]. Therein, the magnetic force between stator and rotor was generated to balance with the gravity force. The direction of the gravity and magnetic forces are different. Therefore, an auxiliary passive magnetic bearing must be used to limit the working position. There are two couple forces cause the system to be unbalanced.

Additionally, one of the drawbacks, which renders the axial magnetic bearing challenging to be implemented in practical applications, is the spontaneous radial levitation force with a positive stiffness coefficient. The radial levitation force simultaneously increases as the axial force rises, and conversely. In the case of passive magnetic bearing, the radial levitation force is tightly depended on rotor and stator operating positions, typically defined by the eccentricity r. However, it is impossible to completely exclude the radial levitation force in axial passive magnetic bearings, yet, strategies to increase the radial-to-axial force ratio are remained achievable, this outlines a potential research direction. With the aim of finding an optimal design for both axial and radial levitation forces, a recent research shown in [14] has made an examination comparing four popular axial magnetic bearings. The experimental results shown the design using a pair of magnets for each radial and axial direction achieves the highest efficiency in force generation. That results in the radial-to-axial force ratio $k = 0.03$, while the radial force generation density is approximately 0.0007 N/mm^3. On another research presented in [15], a conventional magnetic bearing was evaluated for Flywheel application. The evaluation outcome has also provided the radial-to-axial force ratio and the radial force generation density, which respectively are 0.291 and 0.0022 N/mm^3. However, there exists a limitation in these mentioned configurations, is that the magnetic bearing must withstands the demagnetizing stresses occurring from the magnets interactions. Therefore, it is demanding for the magnetic bearing to remain a stable operating position in long term. In addition, besides from being complicated and bulky, these designs also require utilizing a pair of passive magnetic bearings for limiting the axial position.

In this paper, a novel design of the passive magnetic bearing is introduced with the aim of generating both push and pull forces. Therefore, only one bearing is requested for stabilizing the rotor. In this case, the couple forces in two tips of the rotor is removed. Concurrently, the proposed magnetic

bearign configuration allows the constraint of unsought radial levitation forces. Furthermore, together with the reduction of demagnetization between magnets, the closed magnetic circuit is easily obtained in this configuration. Additionally, due to the small dimension of the proposed passive bearing, it can effortlessly integrate with the active bearing in order to control the position along both axial and radial directions.

The structure of this paper is as follows: First, a novel passive magnetic bearing design is introduced and the fundamental principle of bearing force generation is analyzed. Second, a simulation model is developed in Ansys Maxwell to validate the accuracy of the proposed bearing concept and evaluate its performance. Finally, the conclusion is given in the last.

2. Design of the proposed passive magnetic bearing

Herein, the structure and working principle of the proposed passive magnetic bearing are given. Furthermore, an approach to analysis and calculate the radial and axial forces is presented.

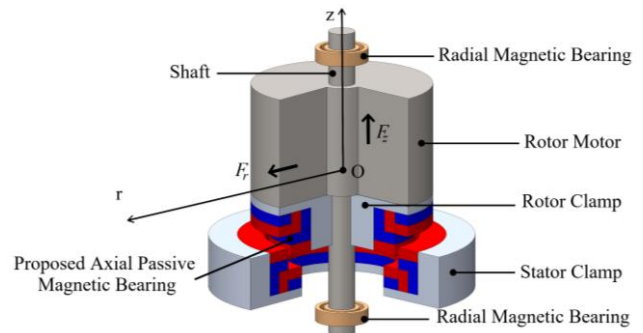### 2.1 Structure of the proposed passive magnetic bearing

Figure 1: The structure of the self bearing motor with support of the proposed passive magnetic bearing
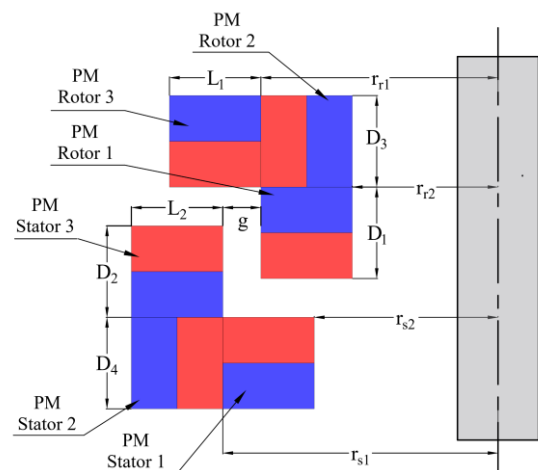

Figure 2. Structure and dimension of magnets in the proposed bearing

In self-bearing motor, the rotor is required to rotate without any mechanical contact to the stator. The requirement of the noncontact along the radial and axial directions must be fulfilled. In figure 1, the self bearing motor with *Or* axis is

controlled by two radial bearings. Herein, the proposed magnetic bearing controls the rotor position along Oz axis. The structure of the proposed bearing is shown in figure 2.

The proposed bearing consists of two main parts. The rotary part is embedded on the rotor of the motor and the stationary part is embedded on the stator of the motor. Therein, the stationary part consists of 3 ring shape magnets with two of them has axial flux direction and one magnet with the radial flux distribution. Similarly, the rotary part consist of the same number of magnets with two axial flux distribution magnets and one radial flux distribution magnet. The centers of the rotor of the motor and rotary part of bearing are the same. For softening the effects of the demagnetization in long time operation, the magnets with the same pole require indirectly alignment. As shown in figure 2 r_{r1}, r_{r2}, r_{s1}, r_{s2} are dimensions of the outer and inner magnet poles of rotory and stationary parts, respectively. D_1, D_2, D_3, D_4 are thicknesses along Oz axis of the magnet rotor 1, magnet stator 3, pair magnets rotor 2 and rotor 3, and pair magnets stator 1 and stator 2, respectively. L_1, L_2 are the width magnets rotor 3 and stator 3.
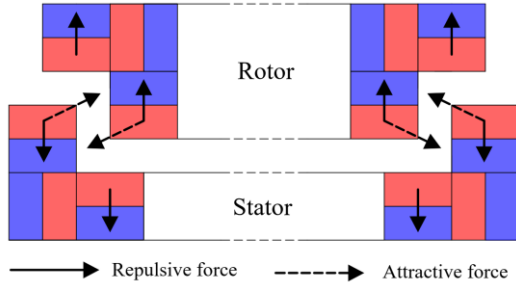

Figure 3. Repulsive and attractive force in proposed APMB

For the propose magnetic bearing design, the interaction forces between magnets are illustrated as in Figure 3. Expressly, the attractive force pairs are formed at the rotor magnet 1 and stator magnet 3 surfaces, while the repulsive force pairs are generated on the surfaces of rotor and stator PM1, PM3 pairs. At the same time, with the aim of minimizing the impact of the magnetic bearing on external devices and improving the magnetic durability of the magnets, the magnet PM2 of rotor and stator plays a role in directing and completing the magnetic circuit for respective configuration. At the operating point where the attractive and repulsive forces are equal, balance point of the system can be determined.

The passive magnetic bearings are sensitive to the designed dimensions such as the direction of the magnetization, positions of the magnets, and its dimensions. Furthermore, the levitation force and its stiffness are strongly depended on the dimensions of the magnets. To obtain the desired flux distribution and avoid the magnetization due to the interact of the magnets, the hard stiffness magnets are highly recommended. In the next section, a theoretical analysis is given for the calculation background of the proposed scheme together with the force generation principle is also shown.

2.2 Working principle

Basically, the energy domains are generated based on the flux linkage lines of the magnets. In the volumes of rotory, stationary, and air gap of these parts, energy domain is highly converged in these mentioned areas. In this case, the rotory and stationary parts are moved in compare to each others, the energy area is variated. Therefore, magnetic field energy in the air gap is then changed accordingly, which is a main reason for the levitating force generation. We have

$$dW_e = dW_f + dW_l + dW_m \tag{1}$$

Where dW_f is the varied magnetic storaged energy of the magnets. The varied loss energy is dW_l, and varied mechanical energy is dW_m. In the passive magnetic bearing, the varied mechanical energy is attractive and repulsive forces of the stationary and rotory parts. Otherwise, the varied electric energy $dW_e = 0$. By assuming that the loss is negligible, the varied energy is then mainly counted for the mechanical energy, which is the source of forces. Therefore

$$dW_f = -dW_m \tag{2}$$

This paper proposes the magnetic bearing with the cylinder shape magnets. Therefore, the directions of the movements of the bearing are along the Oz and Or axes. The forces can be calculated by

$$\begin{cases} F_z = -\partial W_f(z,r)/\partial z \\ F_r = -\partial W_f(z,r)/\partial r \end{cases} \tag{3}$$

The magnet can be considered as the current or charger model. However, the charger model approach is not suitable for complicated bearing shapes. Therefore, the current model and magnetic analysis are used in this paper. Therein, permagnent magnets of the rotory part is modeled equivalently to the magnetomotive force $\mathcal{F}_1$, $\mathcal{F}_2$, $\mathcal{F}_3$ and reluctance $\mathfrak{R}_1$, $\mathfrak{R}_2$, $\mathfrak{R}_3$. Similarly the magnets of the stationary part is considered as magnetomotive force $\mathcal{F}_4$, $\mathcal{F}_5$, $\mathcal{F}_6$ and reluctance $\mathfrak{R}_4$, $\mathfrak{R}_5$, $\mathfrak{R}_6$.
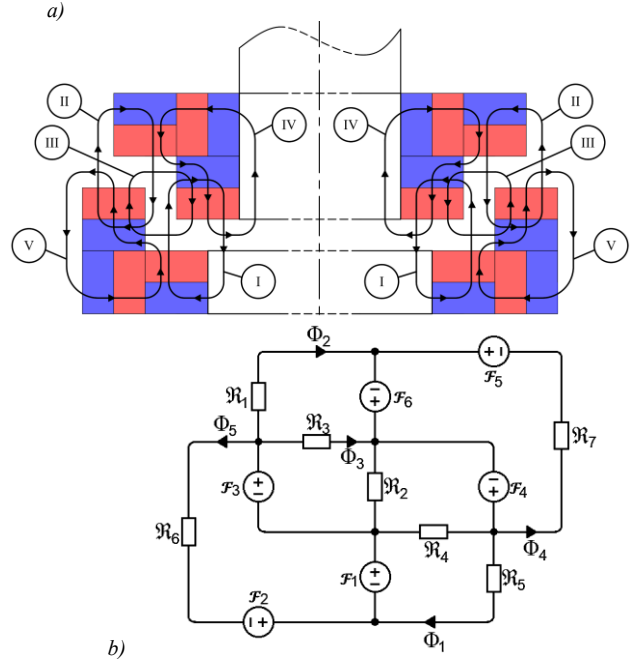

Figure 4: a) Flux lines b) equivalent magnetic circuit of the proposed magnetic bearing

The flux distribution of the proposed magnetic bearing is shown in figure 4a. There are 5 flux lines with line I is the closed flux line of magnet rotor 1 and stator magnet 1. Line II is the closed flux line of magnet rotor 3 and stator magnet 3. Line III is the closed flux line of magnet rotor 1 and stator magnet 3. Line IV is the closed flux line of magnets rotor 1, 2, and 3. Finally, line V is the closed flux line of stator magnets 1, 2, and 3. On the other hand, the magnetic bearing with fully embedded radial and axial forces, it is also required simplicity in installation and fabrication.

Herein, the bearing was designed based on the requirement of $D_1 = D_2 = D$ and $L_1 = L_2 = L$. We have

$$\Re_1 = \frac{z+D}{\pi(g+r)(g+r+2r_{r1}+2L)} \tag{4}$$

$$\Re_2 = \frac{(z+D)}{\pi\left[(g+r)^2 + \left(r_{s1}^2 + 2r_{r1}(g+r) - r_{r1}^2\right)\right]} \tag{5}$$

$$\Re_3 = \Re_4 = \frac{1}{2\pi z} \ln\left(1 + \frac{g+r}{2r_{r1}}\right) \tag{6}$$

$$\Re_5 = \frac{z+D_4}{\pi\left(r_{s2}^2 - r_{r2}^2\right)} \tag{7}$$

$$\Re_6 = \frac{D_2 + D_4}{A_7} \tag{8}$$

$$\Re_7 = \frac{D_1 + D_3}{A_8} \tag{9}$$

where A_7 and A_8 are surface areas of the outer and inner of the bearing, respectively. These values are constant. z and r are movements of the air gaps along the axial and radial directions. The total air gap energy is calculated by

$$W = \frac{1}{2}\sum_{i=1}^{7}\Re_i \Phi_i^2 \tag{10}$$

Due to the reason that the magnetic system is nonlinear, the force is difficult to obtain by using the Eq. (3). Furthermore, the distribution of the flux in the air gap is uneven. To obtain the varied energy, the assumption that the system is working at the position of (z_0, r_0).

$$dW = \frac{1}{2}\sum_{i=1}^{7}\left(d\left(\Re_i \Phi_i^2\right)\right) = \frac{1}{2}\sum_{i=1}^{7}\left(d\left(d\Re_i \Phi_{i0}^2 + \Re_{i0} d\Phi_i^2\right)\right) \tag{11}$$

Otherwise, the varied flux is much smaller than varied reluctance $d\Phi_i^2 \ll d\Re_i$. Therefore, the forces along the axial and radial directions at (z_0, r_0) are calculated as follows:

$$\begin{cases} F_z = -\frac{\partial W_f(z,r)}{\partial z} = -\frac{1}{2}\sum_{i=1}^{7}\left(\Phi_{i0}^2 \frac{\partial \Re_i}{\partial z}\right) \\ F_r = -\frac{\partial W_f(z,r)}{\partial r} = -\frac{1}{2}\sum_{i=1}^{7}\left(\Phi_{i0}^2 \frac{\partial \Re_i}{\partial r}\right) \end{cases} \tag{12}$$

Therefore,

$$F_z = \frac{\left(\Phi_{30}^2 + \Phi_{40}^2\right)}{2z^2\pi}\ln\left(1 + \frac{g+r_0}{2r_{r1}}\right) - \frac{\Phi_{50}^2}{2\pi\left(r_{s2}^2 - r_{r2}^2\right)}$$
$$- \frac{\Phi_{10}^2}{2\pi(g+r_0)\left((g+r_0)+2r_{r1}+2L\right)}$$
$$- \frac{\Phi_{20}^2}{2\pi\left[(g+r_0)^2 + \left(r_{s1}^2 + 2r_{r1}(g+r_0) - r_{r1}^2\right)\right]} \tag{13}$$

$$F_r = \frac{\Phi_{10}^2(z_0+D)}{\pi}\left(\frac{g+L+r_{r1}+r}{(g+r)^2(g+2r_{r1}+2L+r)^2} - \frac{g+L+r_{r1}-r}{(g-r)^2(g+2r_{r1}+2L-r)^2}\right) +$$

$$\frac{\Phi_{20}^2(z_0+D)}{\pi}\left(\frac{g+r_{r1}+r}{\left[(g+r)^2 + \left(r_{s1}^2 - r_{r1}^2 + 2r_{r1}g + 2r_{r1}r\right)\right]^2} - \frac{g+r_{r1}-r}{\left[(g-r)^2 + \left(r_{s1}^2 - r_{r1}^2 + 2r_{r1}g - 2r_{r1}r\right)\right]^2}\right)$$

$$- \frac{\left(\Phi_{30}^2 - \Phi_{40}^2\right)}{2\pi z_0}\frac{2r_{r1}+g}{\left(2r_{r1}+g\right)^2 - r^2} \tag{14}$$

From Eq. (13), the levitation force along z-axis exists one working position where $F_z = 0$ and F_z is negatively proportional to the z movement. This proves that the forces of the proposed bearing consists of the radial and axial forces, which are depended on the position of the bearing along the z axis. Besides, the stiffness of the levitation force is strongly depended on the the air gap dimension. The stiffness is a proportional calculation of the air gap. The equivalent position of the z axis is depended on both the air gap and the length L of the air gap. As shown in Eq. (14), the undesired radial levitation force is proportional to the radial displacement r, it also depends on the flux magnitude produced by two magnetic circuits III. Nevertheless, with the proposed magnetic bearing, the emergence of magnetic circuits I and II generated reverse radial levitation forces, which contributes to a subtantial enhancement of the radial-to-axial force ratio. Moreover, the radial force is proportional to the thickness D of the magnet. This allows a compact design in thickness, in which a high axial levitation force is achieved, whereas the radial lift force is relatively low, which can be easily inserted into self bearing motor.

The air gap and length are small helps reduce the radial force. However, the axial force is then also reduced. In the next section, the simulation in FEA is given to show the precision of the proposed bearing and provide optimization of the thickness of the magnets to obtain a better bearing.

3. FEA simulation results and evaluation

3.1 Simulation results

To test the force of the proposed bearing, the model of the proposed bearing is given in the figure 5 and its parameters are shown in the Table 1. The simulation is obtained by using the Ansys Maxwell software, which is shown in figure 5. The simulation is carried out using the following parameters: maximum element length is 5mm, total number of elements

122.000, maximum number of passes are 100, percent error is 1%, refinement per pass is 30%, nonlinear residual is 0.001.

Table 1. The parameters of the proposed bearing

Parameter	Symbol	Value
Outer dimension of magnet rotor 1	r_{r1}	30mm
Inner dimension of magnet rotor 1	r_{r2}	20mm
Outer dimension of magnet stator 1	r_{s1}	35mm
Inner dimension of magnet stator 1	r_{s2}	25mm
Thickness of magnet rotor 1	D_1	5mm
Thickness of magnet stator 3	D_2	5mm
Thickness of magnet rotor 2 and 3	D_3	2mm
Thickness of magnet stator 1 and 2	D_4	2mm
The width magnets rotor 3	L_1	5mm
The width magnets stator 3	L_2	5mm

Figure 5: The proposed passive magnetic bearing in FEA

The principle of radial and axial forces will be examined accordingly to the changing of the thickness D, the width L and the air gap g, respectively.

3.1.1 Case 1: Effect of Thickness D on Axial and Radial Forces

The axial force is shown with the varying thickness with the step of changing is ΔD and is equal to 1 (mm) from D is equal 4 (mm) to 10 (mm).

As shown in figure 6, the levitation force F_z and stiffness k_z of the bearing is inversely proportional to z. When the thickness D is reduced, the force will increase and it will gradually reduce when the thickness is increased. The stiffness is maximum at $F_z = 0$ and $z_{cb} = 1.5$ (mm). While, the force F_r and stiffness k_r are proportional to the thickness D as shown in Eq. (14). Under each thickness, the stiffness of the radial force is negligible.
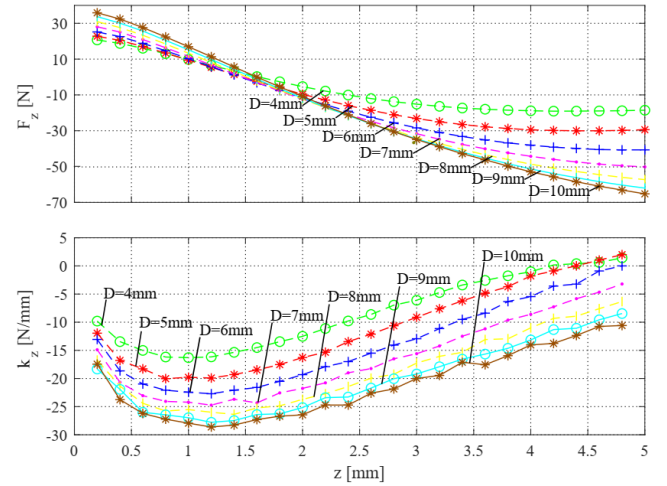

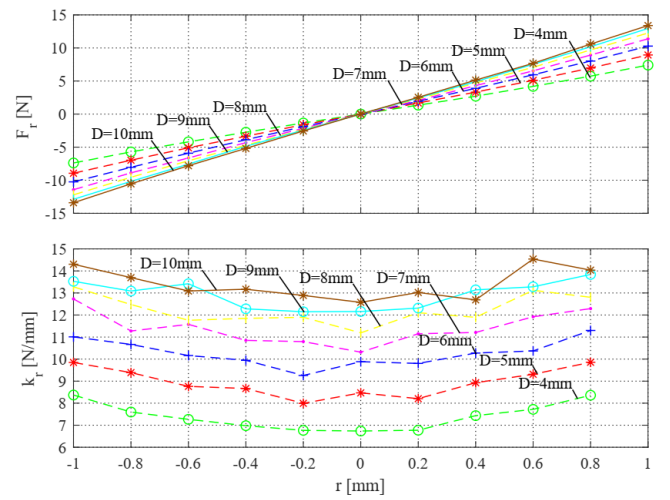**Figure 6:** F_z and k_z under consideration of the varying thickness D

Figure 7: F_r and k_r under variations of thickness D

3.1.2 Case 2: Effect of Air gap g on Axial and Radial Forces

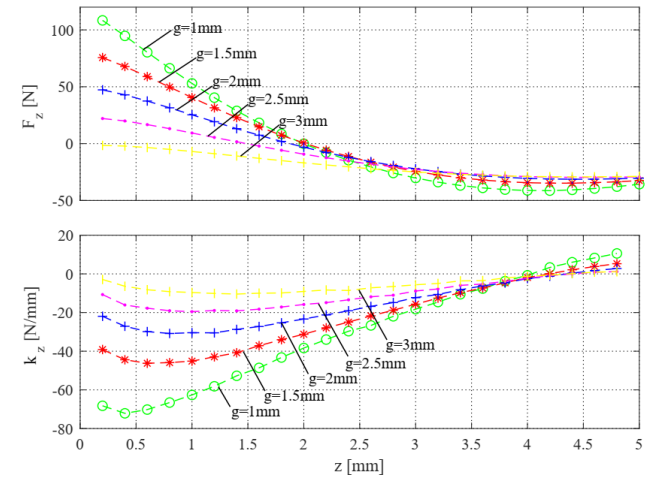Axial force is examined with the range of air gap from 1 (mm) to 3 (mm) under the step size of 0.5 (mm).

Figure 8. F_z and k_z under variations of the air gap g

As shown in figure 8, the axial force and stiffness of the passive magnetic bearing are inversely proportional to z. The force is strongly variated with the small air gaps and vice

versa. Stiffness varies greatly under a small air gap and slightly under a large air gap.
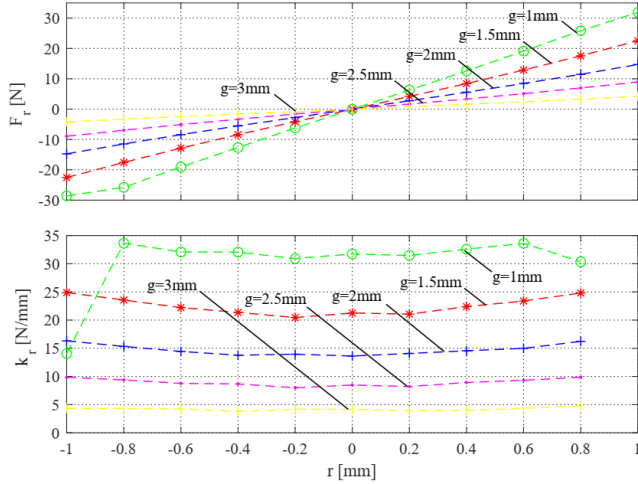

Figure 9. F_r and k_r under variations of the air gap g

As show in figure 9, the radial force F_r and stiffness k_r are inversely proportional to the air gap g. K_r is highly reduced when the air gap g is increased. K_r is hard with the reduction of the air gap.

3.1.3 Case 3: Effect of Thickness L on Axial and Radial Forces

The variations of the width is considered from $L = 4$ (mm) to 11 (mm) and step of changing is $\Delta L = 1$ (mm).
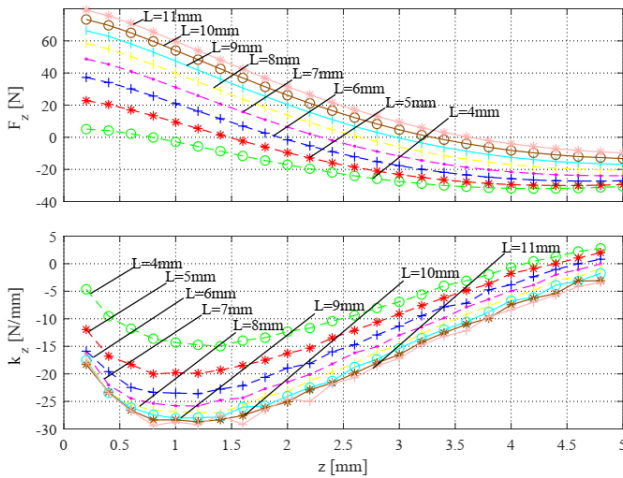

Figure 10. F_z and k_z under variations of the width L

As shown in figure 10, the axial force F_z and stiffness k_z are inversely proportional to the z. The force dramatically changes with small L from 4 to 8 (mm) and gradually reduces with the increase of the width from 9 to 11 (mm). Furthermore, the changing of width L leads to the stiffness is saturated at L is equal to 10 (mm). As shown in figure 11, the radial force F_r and stiffness k_r have huge variations with the width from 4 to 5 (mm). Afterward, the saturation tendency is started with the width from 6 to 11 (mm). Besides, the stiffness is fast reducing when the width is small and reaches the saturation state when the L is reaching 10 (mm).
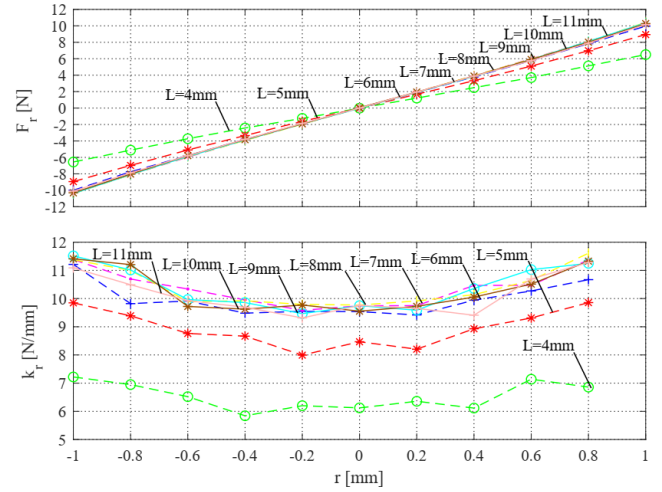

Figure 11. F_r and k_r under variations of the width L

3.2 Evaluation

From the attained FEA simulation result, there exists a range of optimal parameter values as follows: D = 5-7 mm, g = 1-2 mm, L = 6-8mm. With these parameters, the maximum axial and radial levitation forces obtained respectively are 97N and 21N, 25N/mm for the maximum radial stiffness and the total volume of magnets is minimized to 11000 mm^3.

As shown in figures above, the levitation force depends not only on working position, it also depends on the design parameters. The affect of L and g to the stiffness is given in the figure 12. Therein, the magnitude of the stiffness is maximum when the L is high and g is small. Therefore, the change of g to obtain the force is priority.
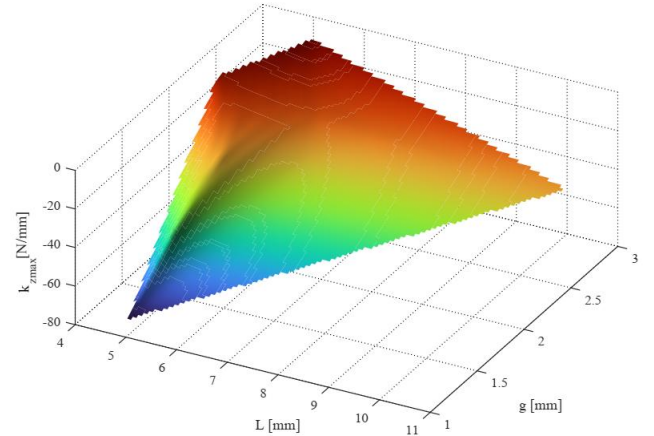

Figure 12. k_{zmax} under variations of the width L and the air gap g

However, the stiffness of the radial and axial forces are the same such shown in figure 13. This problem must be taken into account when the magnetic bearing is designed especially as the active magnetic bearing system.
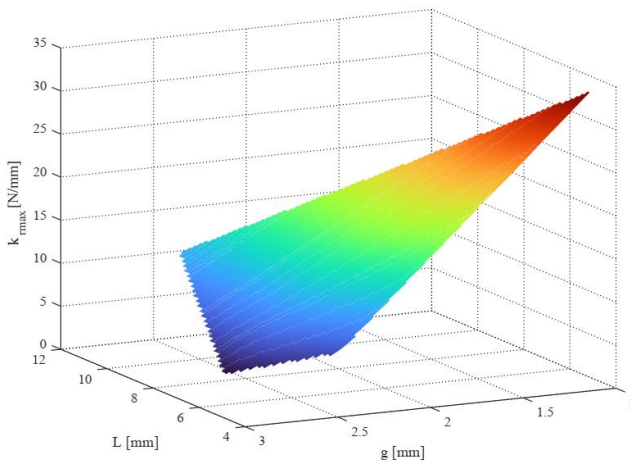
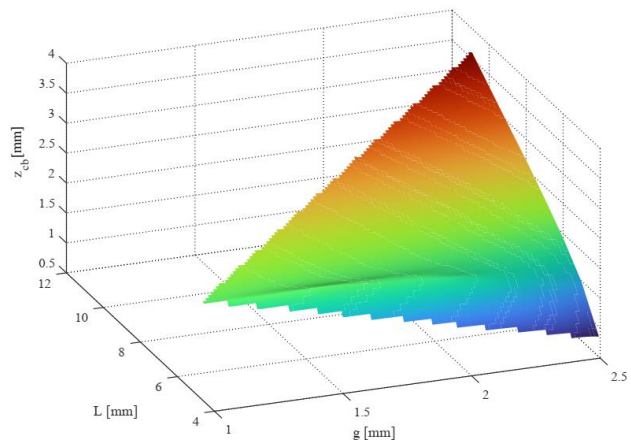**Figure 13.** k_{rmax} under variations of the width L and the air gap g

Figure 14. The equilibrium position z_{cb} under variations of the width L and the air gap g

Therein, the equilibrium position is a requirement in designing the magnetic bearing. As shown in figure 14, the equilibrium is depended on the L and g. The changing of the equilibrium position can be easily obtained by varying the width L.

4. Conclusion

This paper presented a new passive magnetic bearing system which has the ability to generate both push and pull forces along the axial axis. In this proposed bearing design, the equilibrium can be variated. Furthermore, the mathematical operations of the radial and axial forces were given, which clearly shown the relationships between the force and the design parameters of the bearing. The simulation of FEA was used to conduct the power and effectiveness of the proposed bearing. The simulation result shown that the air gap variation is more effective than the other in changing the stiffness of the axial force. Moreover, the equilibrium point can be effectively regulated by changing the width of the magnets.

Acknowledgement

References

[1] Okada, Y., Konishi, H., Kanebako, H., & Lee, C. W. (2000). Lorentz force type self-bearing motor. In Int Symposium on Magnetic Bearings. Seventh International Symposium on Magnetic Bearings.

[2] Nguyen, Q. D., & Ueno, S. (2010). Analysis and control of nonsalient permanent magnet axial gap self-bearing motor. IEEE Transactions on Industrial Electronics, 58(7), 2644-2652.

[3] Baumgartner, T., Burkart, R. M., & Kolar, J. W. (2013). Analysis and design of a 300-W 500 000-r/min slotless self-bearing permanent-magnet motor. IEEE Transactions on Industrial Electronics, 61(8), 4326-4336.

[4] Ishikawa, T., Matsuda, K. I., Kondo, R., & Masuzawa, T. (2009). 5-DOF controlled self-bearing motor. *Journal of System Design and Dynamics*, 3(4), 483-493.

[5] Nguyen, Q. D., Shimai, N., & Ueno, S. (2010, August). Control of 6 degrees of freedom salient axial-gap self-bearing motor. In *12th International Symposium on Magnetic Bearings*.

[6] J. G. Bai and L. M. Wang, "A Flywheel Energy Storage System with Active Magnetic Bearings," *Energy Procedia*, vol. 16, p. 1124, 2012.

[7] Vu, D. D., Nguyen, Q. D., & Nguyen, H. P. (2020). Phân tích và so sánh các cấu trúc ổ từ 4 cực kiểu lai hai bậc tự do. Journal of Measurement, Control, and Automation, 1(2).

[8] A. V. Filatov and E. H. Maslen, "Passive magnetic bearing for flywheel energy storage systems," in *IEEE Transactions on Magnetics*, vol. 37, no. 6, pp. 3913-3924, Nov. 2001

[9] S. Earnshaw, "On the Nature of the Molecular Forces which Regulate the Constitution of the Luminiferous Ether," pp. 97–114, 1842

[10] Y. Dong, S. Ueno and C. Zhao, "Evaluation of Support Stiffness of a Permanent Magnet Attractive Force Type Passive Magnetic Bearing," *2024 27th International Conference on Electrical Machines and Systems (ICEMS)*, Fukuoka, Japan, 2024

[11] M. Van Beneden, V. Kluyskens and B. Dehez, "Optimal Sizing and Comparison of Permanent Magnet Thrust Bearings," in *IEEE Transactions on Magnetics*, vol. 53, no. 2, pp. 1-10, Feb. 2017

[12] Yonnet, J. P. (2003). Passive magnetic bearings with permanent magnets. *IEEE Transactions on magnetics*, 14(5), 803-805.

[13] Fang J, Wang C, Tang J. Modeling and analysis of a novel conical magnetic bearing for vernier-gimballing magnetically suspended flywheel. *Proceedings of the Institution of Mechanical Engineers, Part C: Journal of Mechanical Engineering Science*. 2013;228(13):2416-2425

[14] Nielsen, K. K., Bahl, C. R. H., Dagnaes, N. A., Santos, I. F., & Bjørk, R. (2020). A passive permanent magnetic bearing with increased axial lift relative to radial stiffness. IEEE Transactions on Magnetics, 57(3), 1-8.

[15] Han, B., Zheng, S., Le, Y., & Xu, S. (2013). Modeling and analysis of coupling performance between passive magnetic bearing and hybrid magnetic radial bearing for magnetically suspended flywheel. *IEEE Transactions on Magnetics*, 49(10), 5356-5370.